FABRICATION AND TENSILE PROPERTIES OF ULTRAFINE GRAINED STEELS

D. H. SHIN[a], W. G. KIM[a], J. Y. AHN[a], K. -T. PARK[b] and N. J. KIM[c]

[a] Department of Metall. and Mater. Sci., Hanyang University, Ansan 425-791, Korea
[b] Division of Advanced Mater. Sci. & Eng., Hanbat National University, Taejon 305-719, Korea
[c] Department of Mater. Sci. and Eng., Pohang University of Science and Technology, Pohang 790-784, Korea

ABSTRACT

Three types of ultrafine grained (UFG) low carbon steel were fabricated by equal channel angular pressing, and their microstructure and tensile properties were examined. UFG ferrite/pearlite steels with or without vanadium exhibited ultrahigh strength, almost three times compared to that of their coarse grained counterparts, but their strain hardenability and ductility were drastically degraded. It was found that microalloying of vanadium was effective on improving thermal stability of UFG steels. Contrary to UFG ferrite/pearlite steels, UFG ferrite/martensite dual phase steel exhibited an excellent combination of ultrahigh strength, extensive strain hardenability and enhanced ductility. The tensile properties of each type of UFG steel were discussed along with their microstructural characteristics.

KEYWORDS

low carbon steel, ultrafine grains, equal channel angular pressing, microalloying, dual phase steel,
microstructure, tensile properties

INTRODUCTION

Severe plastic deformation (SPD) is an effective top-down approach refining grains of metallic materials down to the sub-μm level [1], so-called ultrafine grained (UFG) materials. As predicted by the Hall-Petch relationship, UFG materials exhibit ultrahigh strength, but their thermal stability and strain hardenability are much inferior to those of the coarse grained counterparts [2]. This article describes fabrication of UFG

low carbon steels with enhanced thermal stability or strain hardenability by equal channel angular pressing (ECAP), a representative model SPD technique. In the first part, the application of ECAP to fabricate UFG ferrite/pearlite plain low carbon steel and its resultant room temperature tensile properties are demonstrated. A combined process of ECAP and heat treatments for fabrication of thermally stable vanadium microalloyed UFG low carbon steel is addressed in the second part. Finally, the strain hardenability of UFG low carbon ferrite/martensite dual phase steel prepared by ECAP and subsequent intercritical annealing is discussed.

1. UFG FERRITE/PEARLITE LOW CARBON STEEL

1.1 Fabrication

A plain low carbon steel (Fe-0.15%C-0.25%Si-1.1%Mn (in wt.%)) was austenitized at 1473 K for 1 hr and then air-cooled. The steel consisted of ~80% ferrite and ~20% pearlite. The mean linear intercept size of ferrite grains and pearlite colonies was ~30 μm. Then, ECAP was conducted at 623 K up to 4 passes. The ECAP die was designed to yield an effective strain of ~1 per pass [3]: the inner contact angle and the arc of curvature at the outer point of contact between channels of the die were 90° and 20°, respectively. During ECAP, the sample was rotated 180° around the longitudinal axis of the sample between each pass, i.e. route C [4]. Tensile tests were carried out using an Instron machine on the tensile samples with a gage length of 25.4 mm at room temperature.

1.2 Microstructure and tensile properties

As shown in Fig. 1, after 4 passes ECAP, ferrite grains (Fig. 1a) were refined to ~0.3 μm and pearlitic cementite (Fig. 1b) was severely deformed. In order to examine the possibility of carbon dissolution from pearlitic cementite during SPD [5], the steel was annealed at 873 K for 1 hr after ECAP. Fig. 2 shows a SEM micrograph depicting precipitation of nanosized cementite particles at UFG ferrite grain boundaries in the vicinity of pearlite colony, providing a strong evidence of carbon dissolution. So, it is certain that, in the as-ECAPed state, ferrite grains in the vicinity of pearlite colony possess supersaturated carbon content.

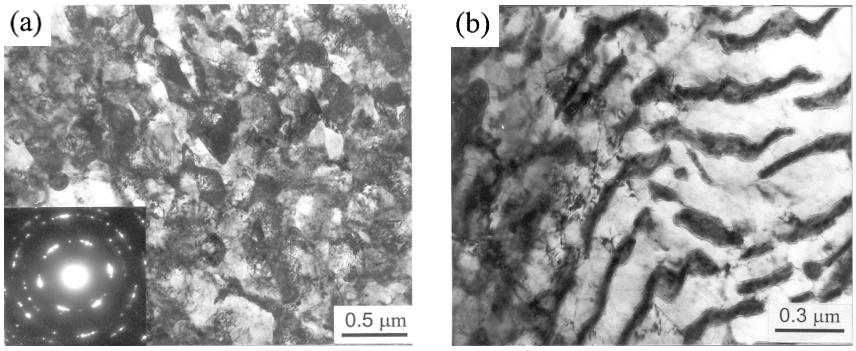

Fig. 1 TEM micrographs of (a) ferrite and (b) pearlite of the present steel after ECAP

Fig. 3 compares the nominal stress-strain curve of the present steel before and after ECAP. Before ECAP, as typical in the ordinary ferrite/pearlite low carbon steels, extensive strain hardening occurred after some extent of yield point elongation. After ECAP, the yield strength was greatly increased, almost three times, but no strain hardening occurred at all and therefore uniform elongation was only few percent. The ultrahigh strength of the as-ECAPed steel can be explained quantitatively by the dislocation bow-out model [6] and the mixture rule. In the dislocation bow-out

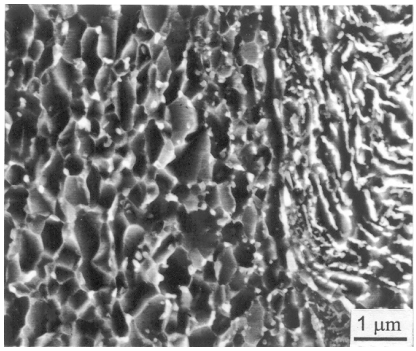

Fig. 2 SEM micrograph showing the precipitation of nanosized cementite particles at UFG ferrite grain boundaries in the vicinity of pearlite colony in the present steel after ECAP followed by 873 K × 1 hr annealing.

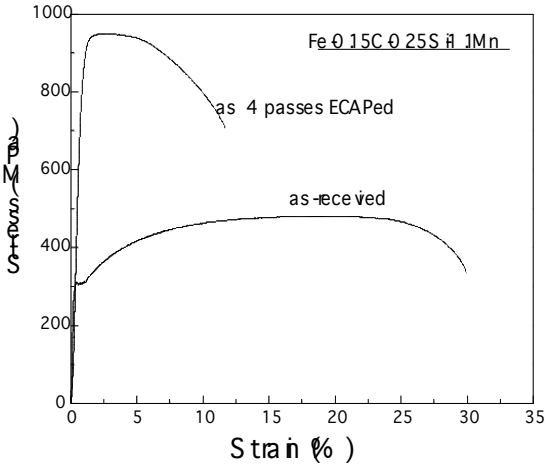

Fig. 3 Representative nominal stress-strain curves of the present steel before and after ECAP

model, the yielding occurs when the dislocation configuration reaches semicircle and the critical stress for such condition is approximated by an expression of

$$\sigma_{critical} = \frac{Gb}{2\pi L(1-\nu)}\left[\left(1-\frac{3\nu}{2}\right)\ln\left(\frac{L}{b}\right)-1+\frac{\nu}{2}\right] \quad (1)$$

where G is the shear modulus, b is the burgers vector, ν is the Poisson's ratio and L is the average dislocation length. For the grain size larger than 100 nm, L is equivalent to $\rho^{-1/2}$ where ρ is the dislocation density. With the aid of Eq. 1, the yield stress of UFG materials can be expressed as

$$\sigma_{YS} = \sigma_o + M\sigma_{critical} \quad (2)$$

where σ_o is the friction stress and M is the Taylor factor.. Using Eqs. 1 and 2, ferrite yield strength of the as-ECAPed steel was estimated as 728 MPa with the following values; G = 78 GPa, b = 2.48×10^{-10} m, ρ = 10^{15} m^{-2}, ν = 0.33, M = 2.78 for BCC structure and σ_o = 76 MPa: usually ρ in several UFG materials manufactured by SPD processes was reported to be in the order of 10^{15} m^{-2} [7]. The present steel consists of ~80% of ferrite phase and the rest of pearlite phase. Therefore, the yield stress of the as-ECAPed steel can be approximated by the mixture rule;

$$\sigma_{YS} = \sigma_{YS}^{f}V_f + \sigma_{YS}^{p}V_p \quad (3)$$

where V is the volume fraction and the superscripts f and p denote ferrite and pearlite, respectively. Due to the lack of information on the application of ECA pressing to pearlitic steel, σ^{p}_{YS} was inferred from that of the cold drawn pearlitic steel. σ^{p}_{YS} of the cold drawn pearlitic steel subjected to the similar effective strain to that used in the present ECA pressing is in the range of 1800 MPa ~ 2000 MPa [8]. From Eq. 3, the yield stress of the present as-pressed steel is about 856 MPa ~880 MPa that is lower than that measured, 937 MPa. This underestimation would be attributed to the two factors: (a) the real dislocation density would be higher than that measured and (b) the effect of internal stress was not considered in the model. Meanwhile, the lack of strain hardening of UFG materials is common and is explained by (a) the grain size is as fine as the dislocation mean free length [2], and (b) under such condition, the dislocation generation rate is comparable to its annihilation rate, i.e. dynamic recovery [9].

2. UFG VANADIUM MICROALLOYED LOW CARBON STEEL

2.1 Fabrication

A vanadium microalloyed low carbon steel (Fe-0.15%C-0.25%Si-1.1%Mn-0.06%V-0.006/0.01N) was oil-quenched to room temperature after the austenitization at 1473 K for 1 hr, and then normalized at 1173 K for 1 hr. The mean linear intercept size of ferrite grain and pearlite colony was ~ 10 μm. This normalized V microalloyed steel was subjected to the identical ECAP described above. In addition, in order to examine the effect of V microalloying on the thermal stability of UFG steel, annealing was conducted for 1 hr in the temperature range of 693 K ~ 873 K.

2.2 Microstructure and tensile properties

The submicrostructure of V microalloyed steel after ECAP was very similar to that of the steel without V as shown in Fig. 1. However, after annealing, the microstructures of the two steels were quite different. An example is shown in Fig. 4. By annealing of 873 K × 1 hr after ECAP, the microstructure of the steel without V (Fig. 4a) consisted of recrystallized coarse ferrite grains and well-defined pearlite colonies. But, by the identical annealing and ECAP, the V microalloyed steel (Fig. 4b) did not reveal pearlite colonies distinctively. Instead, its microstructure was manifested by preservation of UFG ferrite grains and uniform distribution of nanosized cementite particles (Fig. 4c). This unique microstructure is expected to result from the combined effects of V microalloying and severe plastic deformation; that is, (a) the preservation of high dislocation density, providing an effective diffusion path, due to the effect of V addition on suppression of recovery and recrystallization

of the steel [10] and (b) precipitation of fine cementite particles through UFG ferrite matrix via the enhanced diffusion of carbon atoms, which were dissolved from pearlitic cementite by SPD [5], along ferrite grain boundaries and dislocation core.

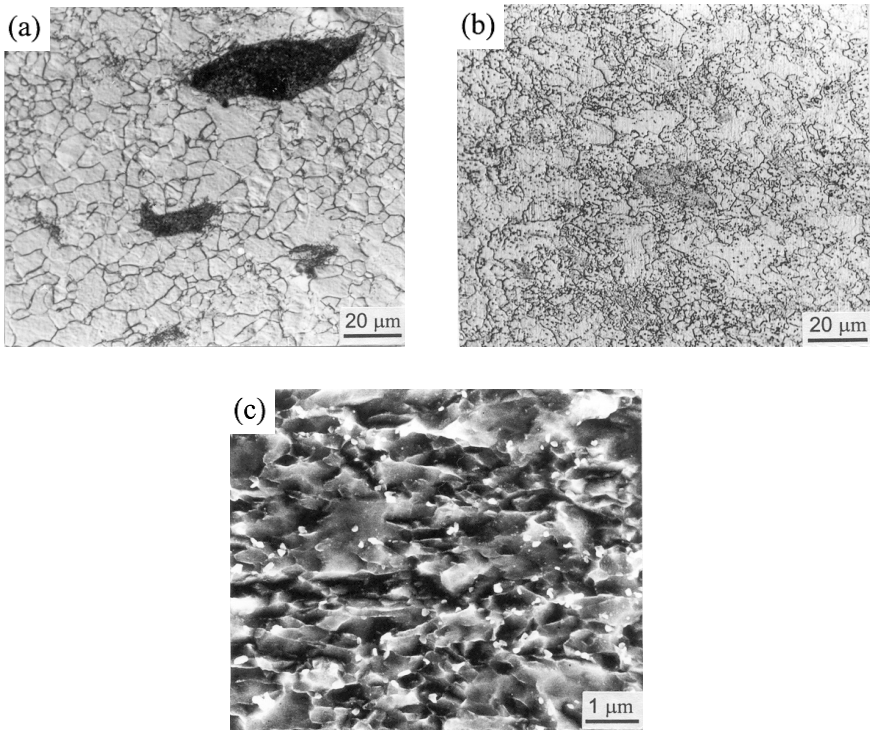

Fig. 4 (a) Optical micrograph of the steel without V after ECAP and annealing at 873 K for 1 hr,
(b) Optical and (c) SEM micrographs of the V microalloyed steel after ECAP and annealing at 873 K for 1 hr.

In Fig. 5, the nominal stress-strain curves of the steel with or without V before and after ECAP are compared. The V microalloyed steel exhibited slightly higher strength with similar strain hardening behavior before ECAP, but no difference of tensile characteristics was made between the two steels after ECAP, indicating the more dominated effect of SPD over V microalloying on the strength. The variation of the tensile properties of the two ECAPed steels as a function of annealing temperature is presented in Fig. 6. While the strength of the steel without V drastically decreased with increasing annealing temperature over ~700 K, the strength loss of the V microalloyed steel was little up to ~800 K. This enhanced thermal stability of the V microalloyed steel is probably attributed to its unique microstructurte aforementioned. However, V addition did not seem to be effective on improving the strain hardenability since the yield ratio (YS/UTS) was over 0.9 even up to ~800 K annealing, as inferred from Fig. 6.

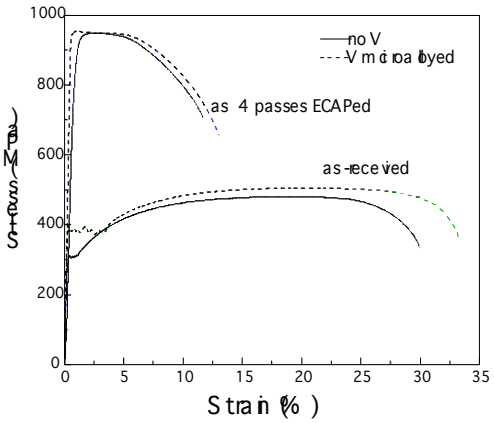

Fig. 5 Representative nominal stress-strain curves of the steels with or without V before and after ECAP

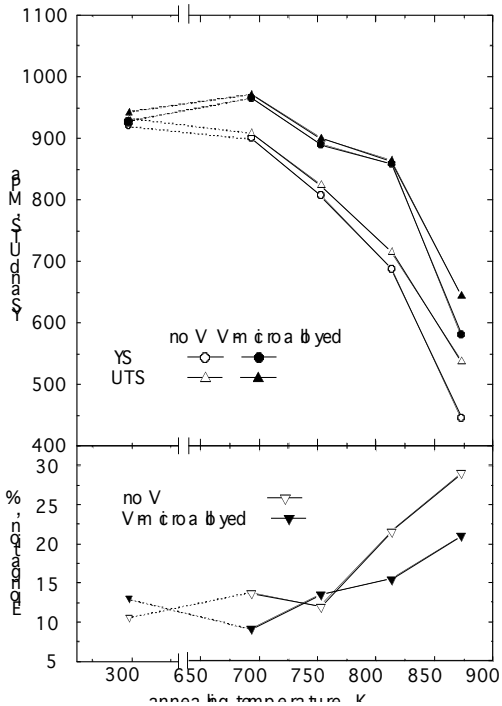

Fig. 6 Comparison of the tensile properties between UFG steels with or without V as a function of annealing temperature (1 hr annealing).

3. UFG FERRITE/MARTENSITE DUAL PHASE LOW CARBON STEEL

3.1 Fabrication

A low carbon steel without V (the same steel described in Section 2) was austenitized at 1473 K for 1 hr and then air-cooled. In order to produce UFG dual phase steel, the steel was subjected to ECAP and subsequent intercritical annealing.

ECAP was conducted up to 4 passes at 500 C. The relatively high ECAP temperature was selected in order to minimize grain growth of retained ferrite during subsequent intercritical annealing. Intercritical annealing of 740 C × 10 min followed by water quenching was undertaken on the ECAPed samples. For the purpose of comparison, coarse grained dual phase steel was prepared by the identical intercritical annealing without ECAP.

3.2 Microstructure and tensile properties

The microstructure of UFG dual phase (UFG-DP) steel consisted of equiaxed ferrite grains and uniformly distributed martensite islands (Fig. 7a). Both ferrite grain size and martensite island size were ~0.8 μm and the martensite volume fraction was about 28 %. Similar to conventional dual phase steels, a very high density of dislocations associated with transformation accommodation was observed in the ferrite grain adjacent to martensite (Fig. 7b). SEM micrograph with higher magnification (Fig. 7c) revealed that martensite was in an isolated blocky type. For coarse grained dual phase (CG-DP) steel (Fig. 7d), the ferrite grain and martensite sizes were ~19.4 μm and ~9.8 μm, respectively, and the martensite volume fraction was about 22 %. The formation of the present UFG-DP microstructure is associated with the fact that the average carbon content in ferrite reached the equilibrium carbon content in austenite at intercritical annealing temperature by diffusion of the carbon atoms dissolved from pearlitic cementite during ECAP. Then, this makes ferrite to be transformed to austenite at its nucleation sites uniformly distributed throughout UFG ferrite matrix during intercritical annealing, and martensite islands is formed from austenite by subsequent quenching.

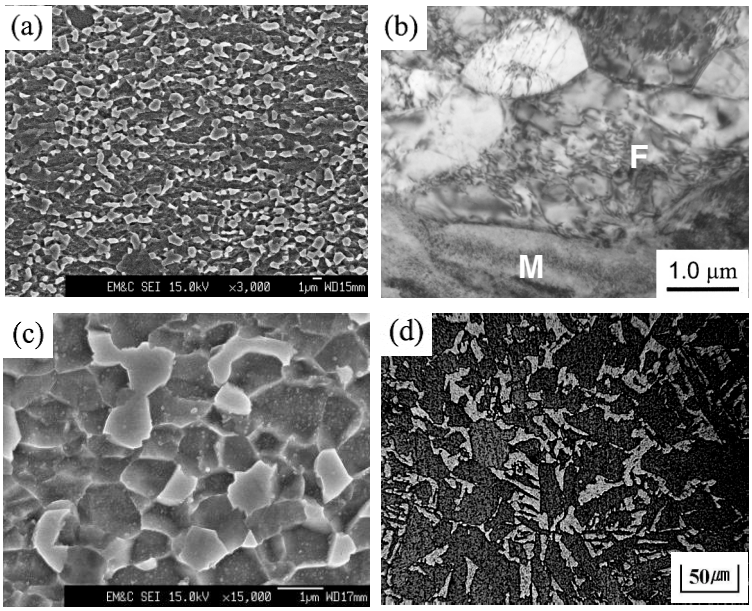

HOME

Fig. 7 (a) SEM micrograph of the present dual phase steel, (a) TEM micrograph of the present dual phase steel, (c) SEM micrograph of the present dual phase steel with higher magnification, (d) Optical micrograph of thecoarse dual phase steel (the white patches are martensite).

The representative nominal stress-strain curves of UFG-DP and CG-DP steels are presented in Fig. 8a. The tensile data of both dual phase steels are listed in Table 1 along with their microstructural parameters. The stress-strain curve of UFG-DP steel is similar to that of CG-DP steel in terms of continuous yielding and rapid strain hardening at the onset of plastic deformation [11]. However, yield strength (σ_{YS}) and ultimate tensile strength (σ_{UTS}) of UFG-DP steel were much higher than those of CG-DP steel in spite of almost the same uniform elongation and even larger elongation to failure. Generally, the strength of dual phase steels linearly increases with increasing the martensite volume fraction (V_m) [12] and obeys the Hall-Petch equation in terms of the ferrite grain size [13]. Accordingly, it is certain that higher strength of UFG-DP steel is attributed to not only ultrafine ferrite grain size but also larger martensite volume fraction than that of CG-DP steel.

Of the analytical methods describing the strain hardening behavior of metals and alloys, the modified Crussard-Jaoul (C-J) analysis based on the Swift equation is known to best describe that of dual phase steels [14]. The Swift σ-ε relationship [15] is expressed as

$$\varepsilon = \varepsilon_o + k\sigma^m \tag{4}$$

where ε and σ are the true strain and stress, respectively, m is the strain hardening exponent, and ε_o and k are material constants. The differentiation of the logarithmic form of Eq. 4 with respect to ε [16,17] gives

$$\ln(d\sigma/d\varepsilon) = (1-m)\ln\sigma - \ln(km) \tag{5}$$

Then, m can be obtained from the slope, (1-m), of the ln ($d\sigma/d\varepsilon$) versus ln σ curve. Such a plot is depicted in Fig. 8b and the m values estimated from the slope of line segments in Fig. 8b are listed in Table 2. Fig. 8b reveals several findings. First, UFG-DP steel exhibited the two stage hardening behavior, as similar to the present CG-DP steel as well as conventional dual phase steels [14]. At the first stage with the low slope, ferrite matrix deforms plastically but martensite remains elastic. At the second stage with the high slope, both phases deform plastically. Second, the m value of UFG-DP steel was higher than that of CG- DP steel at the first stage, but it became comparable at the second stage. The higher m value

of UFG-DP steel at the first stage would be attributed to the fact that plastic deformation of ferrite of UFG-DP steel was more restrained by uniformly distributed martensite islands having smaller interspacing compared to CG-DP steel. Third, the transition strain (ε_{tr}) between the first and second stages was lower in UFG-DP steel, 2.8 %, than that of CG-DP steel, 3.7 %. That is, plastic deformation of martensite in UFG-DP steel started earlier than in CG-DP steel, implying that load transfer from ferrite to martensite in the former was more pronounced than that in the latter [18].

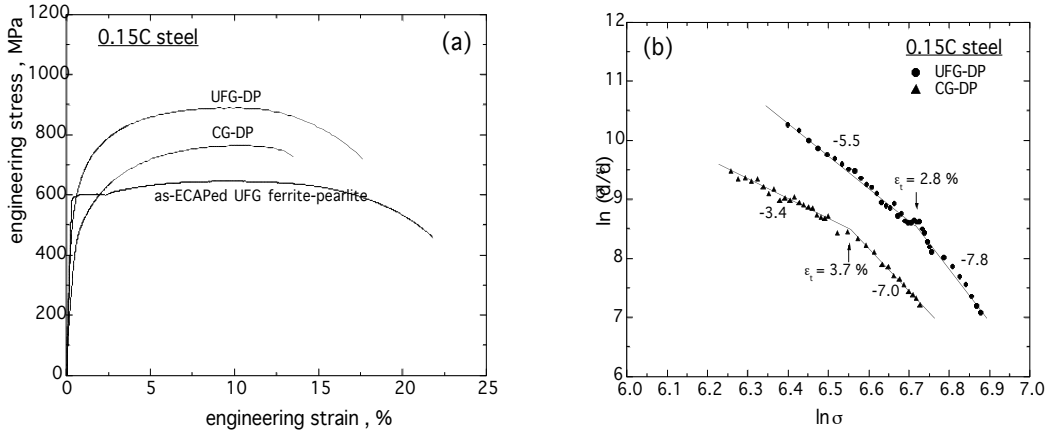

Fig. 8 (a) Comparison of nominal stress-strain curves of the UFG dual phase steel, coarse grained dual phase steel, and UFG ferrite/pearlite phase steel, and (b) Comparison of the plot of the ln ($d\sigma/d\varepsilon$) versus ln σ between UFG-DP and CG-DP steels.

Table 1 Tensile properties of the present DP steels with their microstructural parameters

steels	V_m (%)	d_m (μm)	d_f (μm)	σ_{YS} (MPa)	σ_{UTS} (MPa)	ε_u (%)	e_t (%)	YS/UTS
UFG-DP	28.2	1.3	1.4	581	978	9.3	17.6	0.59
CG-DP	22.1	9.8	19.4	510	843	9.8	13.5	0.60

Table 2 The values of strain hardening exponent of the Swift equation estimated by the modified C-J analysis

steels	first stage	second stage
UFG-DP	6.5	8.8
CG-DP	4.4	8.0

4. SUMMARY

UFG ferrite/pearlite low carbon steels with or without vanadium fabricated by ECAP exhibited ultrahigh strength and disappointingly low ductility and strain hardenabilty, compared to their coarse grained counterparts. But an addition of a small amount of vanadium improved thermal stability of UFG ferrite/pearlite low carbon steel by creating a unique microstructure consisting of UFG ferrite grains with homogeneously distributed nanosized cementite particles. A combined process of ECAP and intercritical annealing resulted in UFG ferrite/martensite dual phase steel exhibiting an excellent combination of ultrahigh strength, enhanced ductility and extensive strain hardenability.

ACKNOWLEDGMENT

This work was supported by a grant (05K1501-00220) from 'Center for Nanostructured Materials Technology' under '21st Century Frontier R & D Programs'

REFERENCES

1) R.Z. VALIEV, R.K. ISLAMGALIEV and I.V. ALEXANDROV, Prog. Mater. Sci. 45, (2000). P.103
2) H. CONRAD, Mater. Sci. Eng. A341, (2003), p.216
3) D.H. SHIN, B.C. KIM, Y.S. KIM and K.-T. PARK, Acta Mater. 48, (2000), p.2247
4) M. FURUKAWA, Y. IWAHASHI, Z. HORITA, M. NEMOTO and T.G. LANGDON, Mater. Sci. Eng. A257, (1998), p.328
5) V. GAVRILJUK, Scripta Mater. 46, (2002), p.175
6) J.P. HIRTH and J. LOTHE, Theory of Dislocations, 2nd ed., Wiley, New York (1982), p.971
7) R.Z. VALIEV, E.V. KOZLOV, Yu.F. IVANOV, J. LIAN, A.A. NAZAROV and B. BAUDELET, Acta Metall. Mater. 42, (1994), p.2467
8) C.M. BAE, Ph.D. dissertation, POSTECH, KOREA (1999)
9) K.-T. PARK, Y.S. KIM, J.G. LEE and D.H. SHIN, Mater. Sci. Eng. A293, (2000), p.165
10) T. GLADMAN, The Physical Metallurgy of Microalloyed Steels, The Institute of Materials, London, (1997), p.213
11) G. KRAUSS, Deformation, Processing, and Structure, ASM, Metals Park, (1982)

HOME

p.47
12) R.G. DAVIS, Metall. Trans. A. 9, (1978), p.671
13) P-H. CHANG and A.G. PREBAN, Acta Metall. 33, (1985), p.697
14) Y. TOMITA and K. OKABAYASHI, Metall. Trans. A. 16, (1985), p.865
15) H.W. SWIFT, J. Mech. Phys. Solids. 1, (1952), p.1
16) C. CRUSSARD, Rev. Metall. 47, (1950), p.589
17) B. JAOUL, J. Mech. Phys. Solids. 5, (1957), p.95
18) Z. JIANG, J. LIAN and J. CHEN, J. Mater. Sci. Tech. 8, (1992), p.1075

HOME